



**Fabrication of Sub-20 nm Patterns using Dopamine Chemistry in Self-Aligned Double Patterni**

Journal:	<i>Nanoscale</i>
Manuscript ID	NR-ART-05-2018-004040.R1
Article Type:	Paper
Date Submitted by the Author:	11-Sep-2018
Complete List of Authors:	Li, Yinyong; University of Massachusetts Amherst, Polymer Science and Engineering Choi, Jaewon; University of Massachusetts Amherst, Polymer Science and Engineering sun, zhiwei; University of Massachusetts, Polymer Science and Engineering Department Russell, Thomas; University of Massachusetts, Polymer Science and Engineering Department Carter, Kenneth; University of Massachusetts-Amherst, Polymer Science and Engineering



## Fabrication of Sub-20 nm Patterns using Dopamine Chemistry in Self-Aligned Double Patterning

Yinyong Li,<sup>a</sup> Jaewon Choi,<sup>a</sup> Zhiwei Sun,<sup>a</sup> Thomas Russell,<sup>a\*</sup> and Kenneth R. Carter<sup>a\*</sup>

Received 00th January 20xx,  
Accepted 00th January 20xx

DOI: 10.1039/x0xx00000x

www.rsc.org/

A self-aligned double patterning approach using a dopamine chemistry - inspired coating technique has been developed for the fabrication of sub-20 nm patterns. Poly (methyl methacrylate) (PMMA) films were patterned by nanoimprint lithography to form relief features. A thin layer of polydopamine (PDA) was conformally deposited on the surface of the PMMA pattern sidewalls to form a spacer layer. After etching the surface of the PDA layer from the horizontal surfaces and subsequently removing the PMMA template, free-standing PDA sidewall patterns remained that essentially doubled the original PMMA pattern density with decreased feature dimensions as compared to the initial PMMA template structures. The critical dimension of the PDA patterns can be tuned to ~ 20 nm by controlling the PDA deposition conditions and further reduced to ~ 13 nm by thermal carbonization of the PDA. Both simple lines and more complex rhombic ring features were fabricated by this technique to demonstrate its capacity for replicating arbitrary patterns. This work represents a simple and scalable strategy for preparing well-defined nanostructures with feature sizes usually only accessible via complex leading edge lithographic methods.

### Introduction

The ability to fabricate nanometer-scale patterns is of crucial importance in nanotechnology. A great deal of progress continues to be made with techniques, such as electron-beam lithography,<sup>1,2</sup> extreme ultraviolet interference lithography,<sup>3,4</sup> block copolymer lithography,<sup>5,6</sup> and nanoimprint lithography,<sup>7,8</sup> however, most of these techniques suffer from either complex multistep processes, reliance on expensive tools and facilities, low process throughput, and the inherent difficulty of methods that can increase pattern density.

Self-aligned double patterning (SADP), also known as spatial frequency doubling or spacer lithography, is a technique capable of fabricating sub-100 nm patterns where the pattern density can be doubled over large areas.<sup>9-12</sup> SADP involves several steps: (1) the deposition of a spacer layer on the sidewall of pre-patterned resist template or mandrel (usually prepared either by photolithography,<sup>13</sup> interference lithography,<sup>14</sup> or nanoimprint lithography<sup>15</sup>); (2) plasma etching of the spacer materials on horizontal surfaces; and (3) removal of the pre-patterned resist template. The spacer mandrel can be formed by several techniques, including material sputtering,<sup>16</sup> and chemical vapor deposition.<sup>11</sup> Atomic layer deposition (ALD, a specific form of chemical vapor deposition) has shown high effectiveness and its utilization is

preferred for spacer lithography, due to the ability to produce uniform conformal coatings with precise control of film thickness.<sup>14, 17-21</sup> A significant limitation is that ALD demands complicated, expensive instrumentations, high purity precursor chemicals and substrates, and extensive removal of excess precursor and reaction by-products. Moreover, depositing films tens of nanometers in thickness by ALD requires hundreds of deposition cycles, resulting in relatively low deposition speeds.<sup>22</sup> While powerful, ALD can only be implemented in laboratories with the resources and overhead to deploy this process. These limitations combine to restrict the broader applications of ALD in SADP.

Mussels, bivalve mollusks, are known to express 3,4-dihydroxy-L-phenylalanine (DOPA) and lysine-enriched proteins to enable tight attachment to surfaces, even in wet aqueous environments.<sup>23</sup> This has inspired researchers to explore similar molecules, dopamine and its derivatives, as functional adhesives and coatings.<sup>24-27</sup> By tuning dopamine concentration in these formulations, uniform polydopamine (PDA) thin films with controlled thicknesses have been conformally deposited on virtually any surface through a one-step coating process.<sup>28-31</sup> The capability to conformally coat PDA thin films isotropically over the periphery of patterned substrates makes this material a viable alternative to ALD layers for spacer lithography. Processes, such as ALD, can be used to form robust, etch resistant films, such as Al<sub>2</sub>O<sub>3</sub>, whereas the high phenolic content of PDA imparts enhanced plasma resistance with properties akin to Novolak resins which are still widely used as photoresists today. PDA can be coated under mildly alkaline conditions at room temperature and does not require costly facilities or high purity chemicals,

<sup>a</sup> Department of Polymer Science and Engineering, University of Massachusetts – Amherst, 120, Governors Drive, Massachusetts, 01003, United States  
Email: Russell@mail.pse.umass.edu; krcarter@polysci.umass.edu.

\*Electronic Supplementary Information (ESI) available: See DOI: 10.1039/x0xx00000x

hence PDA coatings can be considered as an easier way to implement and a more cost-effective conformal coating process than ALD.

In this report, a robust SADP technique is described and used to fabricate sub-20 nm structures on a wafer scale ( $2 \times 2 \text{ cm}^2$ ) using mussel-inspired dopamine chemistry. PMMA thin films were pre-patterned by nanoimprint lithography to form grating structures. After removing the residual PMMA layer in the trench area, a thin layer of PDA was directly deposited onto the surface of the PMMA lines by self-polymerization under mildly alkaline conditions. By etching the top-layer of PDA from the horizontal surfaces and removing the PMMA template, free-standing PDA sidewall patterns were achieved with doubled pattern density and feature sizes of  $\sim 20 \text{ nm}$ . Furthermore, this report demonstrates the use of this dopamine chemistry-inspired SADP in the fabrication of complex and ultrafine rhombic nano-structures.

## Experimental

### Materials

All reagents were used as received unless otherwise specified. Dopamine hydrochloride (99%) and tris(hydroxymethyl)aminomethane (Tris) were purchased from Alfa Aesar (Ward Hill, MA). Ethyl acetate and anisole were purchased from Acros Organics (Morris Plains, NJ). Poly(methyl methacrylate) (PMMA,  $M_w = 75,000$ ) was purchased from Scientific Polymer Products, Inc. Silicon wafers (5 inch, n-type, As doped, [100], thermal oxide  $3.5 \pm 0.5 \mu\text{m}$  thick) were purchased from El-Cat, Inc. A thermally cross-linkable polydimethylsiloxane formulation, Sylgard 184 elastomer mixture kit was purchased from Fisher Scientific (Fair Lawn, NJ).

### Nanoimprint Lithography

Nanoimprint lithography molds consisting of "hardened", crosslinked polydimethylsiloxane elastomer (*h*-PDMS) were replicated from silicon master molds using a previously described method.<sup>32, 33</sup> Silicon wafers were rinsed with hexanes, acetone, and ethanol, and then dried under nitrogen, followed by exposure to oxygen plasma for 5 minutes using a Phantom III ICP reactive ion etcher (RIE) (Trion Technology, Inc). PMMA was spin-coated onto clean silicon wafers from anisole solution (3 wt.% of PMMA) at 3000 rpm for 60 s, which gave a film thickness of  $\sim 59 \text{ nm}$ . The as-spun PMMA films were baked on hot plate at  $100 \text{ }^\circ\text{C}$  for 30 min to remove residual solvent. A Nanonex NX-2000 nanoimprinter was used to imprint PMMA films using *h*-PDMS molds at  $140 \text{ }^\circ\text{C}$  with pressure of 300 psi for 2 min. Residual layers after imprint were removed by mild oxygen plasma (Pressure: 4 mTorr, power: 40 W,  $\text{O}_2$  flow rate: 50 sccm) using a STS Vision 320 RIE System.

### Polydopamine (PDA) coating and etching

The patterned PMMA films (after imprinting and etching) were placed in a dopamine hydrochloride ( $0.4 \text{ mg}\cdot\text{mL}^{-1}$ ) solution at a

pH of 8.5 (10 mM TRIS buffer) for 12 h. The resulting PDA-coated films were then rinsed with deionized (DI) water and dried under nitrogen. The coating process was repeated for a predetermined number of times. Oxygen plasma (pressure: 4 mTorr, power: 40 W,  $\text{O}_2$  flow rate: 50 sccm) was applied to remove the top layer of the PDA film and expose the underlying PMMA lines. The exposed PMMA lines were dissolved in ethyl acetate and the remaining PDA sidewalls were obtained with a pattern density double of the initial PMMA patterns. The PDA lines could be further carbonized at  $400 \text{ }^\circ\text{C}$  under nitrogen for 1 h to achieve size reduced patterns.  $\text{CHF}_3$  plasma etching (pressure: 5 mTorr, power: 150 W,  $\text{CHF}_3$  flow rate: 10 sccm) was used to etch silicon dioxide on the silicon wafers at a rate of  $0.2 \text{ nm}\cdot\text{s}^{-1}$ .

### Characterization

Patterned surface structures were examined by atomic force microscopy (AFM, Digital Instrument, Dimension 3100) in the tapping mode and scanning electron microscopy (SEM, FEI Magellan 400). Fourier Transform Infrared Spectroscopy (FT-IR) spectra were recorded using a PerkinElmer Spectrum 100 FT-IR spectrometer. Transmission spectra were collected in the range of  $650\text{--}4000 \text{ cm}^{-1}$  with resolution of  $4 \text{ cm}^{-1}$ . Film thickness was analyzed using a Veeco Dektak Stylus Profilometer.

Thermogravimetric analysis (TGA) was conducted under nitrogen atmosphere on a TA Instruments TGA Q50. Free PDA for thermal analysis was isolated from the coating solution by centrifuging after the completion of the reaction and dried under vacuum. Dry PDA powder samples were first heated from  $25 \text{ }^\circ\text{C}$  to  $400 \text{ }^\circ\text{C}$  at a heating rate of  $10 \text{ }^\circ\text{C}\cdot\text{min}^{-1}$  and kept at  $400 \text{ }^\circ\text{C}$  for 1 h.

## Results and discussion

PDA film coating conditions on flat silicon wafer substrates were optimized by varying the dopamine concentrations in the deposition solutions. Figure S1a shows a schematic illustration of self-polymerization of dopamine. Under mildly alkaline conditions, dopamine can be oxidized and self-polymerizes into PDA, which forms a thin coating on the surface. The silicon wafers were placed in a dopamine hydrochloride solution with pH of 8.5 (10 mM TRIS buffer) at room temperature for 12 h with stirring. The resulting PDA coated wafers were then rinsed with DI water and dried under nitrogen. The coated surfaces exhibited granular features (Fig. S1 c-f), ascribed to the fact that PDA thin films consist of aggregates of small PDA particles.<sup>29, 34</sup> When the dopamine concentration was increased from  $0.2 \text{ mg}\cdot\text{mL}^{-1}$  to  $0.5 \text{ mg}\cdot\text{mL}^{-1}$ , the film thickness increased from 5 nm to 17 nm and the corresponding root-mean-square (RMS) roughness increased from 1.0 nm to 4.5 nm (Fig. S1b). The films made from lower dopamine concentrations ( $0.3 \text{ mg}\cdot\text{mL}^{-1}$  and  $0.4 \text{ mg}\cdot\text{mL}^{-1}$ ) were similar,

with roughnesses of 1.9 nm and 2.6 nm, respectively. These were significantly smoother than the films formed from 0.5 mg·mL<sup>-1</sup> solutions (4.5 nm). The film thickness of PDA from the 0.4 mg·mL<sup>-1</sup> solution was thicker (13.6 nm) than that of the sample made from 0.3 mg·mL<sup>-1</sup> (10.0 nm). These optimization studies show that targeted thicknesses can be reached more rapidly when coated with 0.4 mg·mL<sup>-1</sup> with a minimal sacrifice in surface roughness and these coating conditions were selected for all subsequent work.

Fig. 1a and 1b show atomic force microscopy (AFM) height images of PDA surfaces after a single (1X) and four (4X) coating steps, respectively. Both surfaces exhibited a similar morphology and the surface roughness increased minimally with increasing number of coatings from 1X (2.6 nm) to 4X (2.3 nm). The PDA layer thickness scaled linearly with the number of coatings while the overall observed roughness remained low with a small increase from 2.3 nm to 5.0 nm (Fig. 1c). The linear relationship between the film thickness and the number of coatings enabled good control of PDA layer thickness, up to ~80 nm, while maintaining a relatively low surface roughness (< 5 nm).

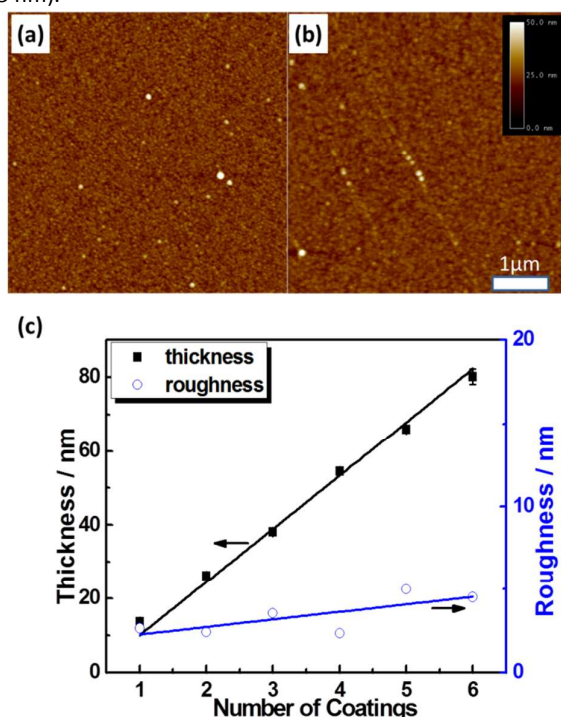


**Fig. 1** AFM surface scan images of PDA surfaces; (a) after a single coating step and (b) after four coating steps. (c) plots of coating thickness and surface roughness as a function of number of coatings.

Fig. 2 illustrates the key steps in the use of dopamine chemistry in the SADP process, including nanoimprint lithography of the PMMA template, plasma etching descumming, PDA coating, breakthrough etching, PMMA template removal, and carbonization of PDA. First, PMMA films (thickness of 59 nm) were coated on silicon substrates

(containing a 3.5 μm silicon oxide layer) and patterned with gratings (line width of 130 nm, pitch size of 260 nm, depth of 110 nm) by nanoimprint lithography using “hardened”, crosslinked polydimethylsiloxane elastomer (*h*-PDMS) molds (Fig. 2a and 2b).<sup>32</sup> Fig. 3a depicts the uniform PMMA grating patterns obtained after nanoimprint lithography. The residual PMMA layer (with estimated thickness around 4 nm) in the trenches was removed to expose the underlying substrate using oxygen plasma etching (Fig. 2c). Next, the patterned PMMA structures were coated with PDA using the same reaction conditions as described above for coating flat substrates (Fig. 2d). The coating step was repeated when thicker PDA films were desired. For example, after two deposition cycles were performed on the PMMA line patterns, a thin conformal layer of PDA was coated onto the surface of the PMMA gratings. The surface of the line patterns became rougher with the observation of PDA nanoparticles on the surface (Fig. 3b, SEM and AFM images).

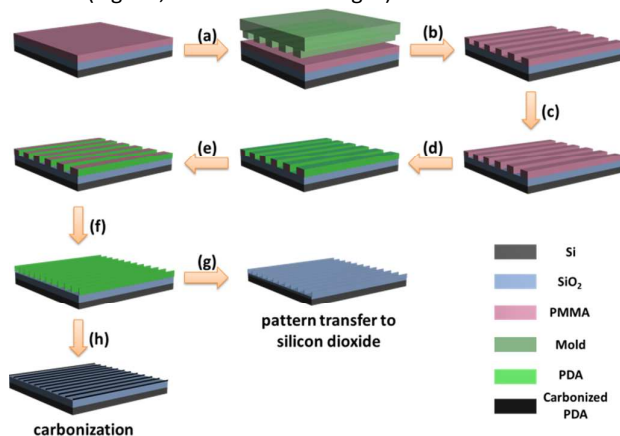


**Fig. 2** Schematics of polydopamine (PDA) in SADP: (a) Nanoimprint on PMMA, (b) demolding, (c) etching residual PMMA from pattern trenches, (d) PDA coating, (e) removal of PDA layers on horizontal surfaces, (f) removal of PMMA template, (g) transferring patterns to silicon dioxide by CHF<sub>3</sub> reactive ion etching, and (h) carbonization of PDA line features.

The PDA conformally coats the entire exposed surface. The portion of the PDA layer on the surface of the PMMA template and trench areas was removed by using a directional anisotropic oxygen plasma etching step, resulting in the exposure of the underlying PMMA template and silicon substrate (Fig. 2e). The exposed PMMA template was then selectively removed by dissolution with ethyl acetate, leaving intact the PDA sidewalls attached to the silicon substrate (Fig. 2f). These PDA sidewall lines effectively doubled the pattern density of the original PMMA lines (Fig. 3c and 3d). The final heights of the PDA lines (~50 nm) were measured by AFM, and SEM was used to determine the width of the PDA lines. The width was found to be ~21 nm (Fig. 3d), which was in good agreement with the thickness of the conformal PDA film (26 nm) originally coated on the surface. The slight reduction of line width is more than likely, due to a partial thinning during

exposure to the oxygen plasma. The height-width ratio (2.5:1) of the lines is similar to the range of 2:1 to 5:1 observed in ALD-based SADP.<sup>17, 19</sup> While the patterns are uniform overall, the line edges show apparent roughness with line edge roughness (LER) of  $\sim 6.11$  nm (Fig. S4), primarily due to particulate protrusions of the PDA coating. The coating condition and process need to be further optimized to decrease the roughness of the coating, so as to reduce LER.

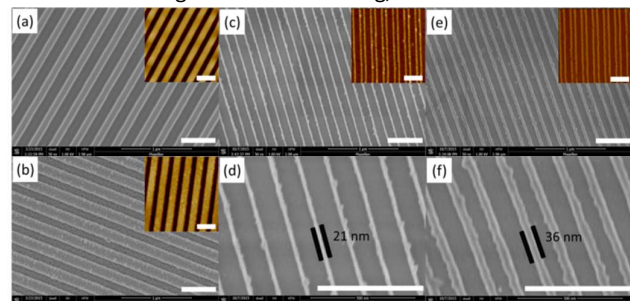


**Fig. 3** Pattern doubling of line gratings via SADP. SEM images of (a) PMMA line patterns created by nanoimprint lithography; (b) PDA coated PMMA patterns; (c) and (d) PDA sidewall patterns with width of  $\sim 20$  nm after removal of the PMMA template; (e) and (f) SiO<sub>2</sub> lines after plasma etching using PDA patterns as mask. The insets are corresponding AFM height images and scale bars represent 500 nm.

The final PDA line features serve as an effective anisotropic plasma resist mask enabling pattern transfer to the underlying silicon oxide substrate by plasma etching with trifluoromethane (CHF<sub>3</sub>) as the gas source (Fig. 2g). The comparative etch rates of PDA, PMMA, and silicon oxide under both O<sub>2</sub> and CHF<sub>3</sub> plasma conditions are shown in Table S1. Under O<sub>2</sub> plasma, PDA exhibits a much higher etch resistance as compared to PMMA. Moreover, the etch rate of PDA (3.7 nm/min) is less than one-half of that of silicon oxide (9.0 nm/min) when exposed to CHF<sub>3</sub> reactive ion etching, indicating that PDA can be used to affect pattern transfer into silicon oxide. Micrographs of the successful pattern transfer into silicon oxide are shown in Fig. 3e and 3f. The height of the patterned silicon dioxide structures is  $\sim 32$  nm (obtained from AFM image, Fig. S3) and the width is  $\sim 36$  nm, which was greater than that of the initial 21 nm PDA mask. The increase in the width is attributed to the tapered etch profile during the plasma etching, a commonly observed effect when etching silicon oxide with CHF<sub>3</sub>.<sup>35</sup>

The conformal coating of PDA in this process, as in SADP with ALD, can be used for pattern doubling and fabricating more complicated nanostructures.<sup>17, 19</sup> For example, a rhombus-shaped pillar pattern (side length around 600 nm, angle of 60° and depth of 150 nm) was used in this sidewall template process to prepare rhombic features. The same steps as with SADP to generate lines were followed, nanoimprint lithography of the PMMA template, clean out etch, PDA deposition, followed by PMMA removal, and CHF<sub>3</sub> etch. The rhombic PMMA pillars made from nanoimprint lithography

had smooth surfaces, as shown in Fig. 4a. After two coatings of PDA, the surface showed granular features (Fig. 4b), similar to those described above. After removing the PMMA template, a well-defined array of rhombic nanostructures was present on the surface (Fig. 4c). Due to the conformal nature of the PDA deposition, the sidewalls of these rhombus ring patterns were around 20 nm. These PDA patterns were used as a mask to etch into the underlying silicon oxide substrate using a CHF<sub>3</sub> plasma. Similar to the line patterns, the silica rhombic structures increased in width to 34 nm during the plasma etching (Fig. 4d). The ability to fabricate the rhombic nanostructures demonstrates that this technique can be applied to prepare other well-defined complex features.

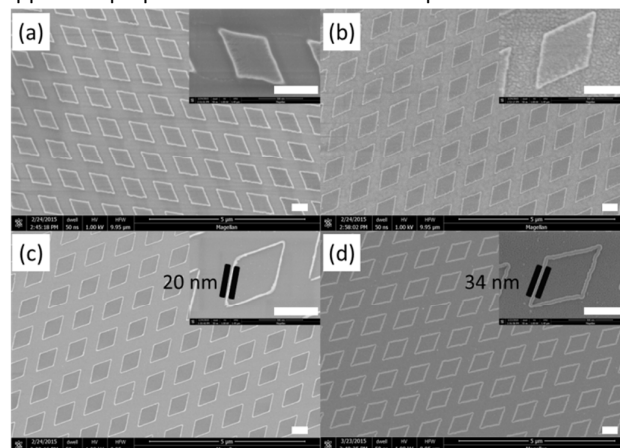


**Fig. 4** Fabrication of rhombus ring patterns via PDA SADP. SEM images of (a) PMMA rhombus patterns by nanoimprint lithography; (b) PDA coated PMMA rhombus patterns; (c) PDA rhombus ring features after removing of PMMA; and (d) SiO<sub>2</sub> rhombus ring patterns prepared by CHF<sub>3</sub> plasma etching using PDA rhombus ring features as mask. Scale bars represent 500 nm.

The minimum feature size that can be achieved is  $\sim 20$  nm using a double coating of PDA. Attempts to further reduce the line width by decreasing the PDA coating thickness led to pattern instability and collapse during the PMMA template removal step. As shown in Fig. S2a, doubled patterns were not observed after a single PDA coating. In these cases, the only patterns remaining on the surface were shallow line features with depths of  $\sim 11$  nm, closely matching the thickness (13.6 nm) of a single PDA coating. This indicates that the remaining structures are the collapsed line patterns. The collapsing of ultrathin (width of  $\sim 11$  nm) line patterns likely results from the capillary forces generated during the dissolution of the PMMA template in ethyl acetate. A similar collapsing phenomenon, indicated by the arrows in Figure S2b, was observed for the rhombic patterns generated from a single PDA coating.

While it was difficult to prepare smaller patterns by reducing the PDA coating thickness, promising results were achieved by carbonizing the PDA under nitrogen. Pyrolysis and carbonizing of PDA under an inert environment has been

shown to nitrogen doped carbon structures.<sup>36-39</sup> Thermogravimetric analysis (TGA) was conducted under nitrogen atmosphere to analyze the carbonization of PDA. The heating of PDA to 400 °C decomposes PDA to give a 29 wt.% char residue (Fig. 5a). As long as this reduction in weight is accompanied by a similar reduction in volume, the PDA line patterns should be suitable for size reduction lithography<sup>40</sup> upon carbonization (Fig. 2h). The FTIR spectra of PDA and carbonized PDA are shown in Fig. 5b. The major bands of PDA spectrum at 3250 cm<sup>-1</sup>, 1500 cm<sup>-1</sup>, and 1280 cm<sup>-1</sup> correspond to stretching vibration of O-H and N-H, aromatic C=C stretching, and stretching vibration of C-N and C-O, respectively. The broad band at 3250 cm<sup>-1</sup> was dramatically reduced after pyrolysis, indicating the loss of the O-H and N-H group between PDA molecules through dehydration. This dehydration was also confirmed by the appearance of a C-O-C stretching band 1250 cm<sup>-1</sup>. The dehydration is a major reaction during the carbonization of PDA and represents a large fraction of the observed weight loss. After heating under nitrogen at 400 °C for 1 h, the PDA line width shrank from 21 nm (Fig. 5c) to around 13 nm and the height decreased from 50 nm to about 18 nm (Fig. 5d). The volume shrinkage was estimated to be 78% based on the observed size reduction after carbonization, which is consistent with the 71% of weight loss observed by TGA.

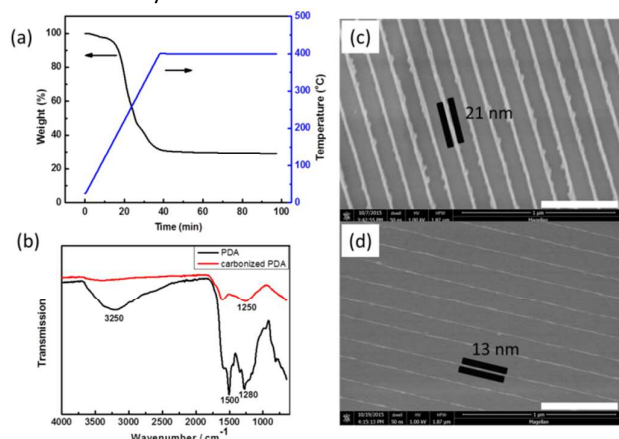


**Fig. 5** Carbonization of PDA: (a) TGA curve of dry PDA powder; (b) FTIR spectra of PDA and carbonized PDA; comparison of PDA line features before (c) and after (d) carbonization. The scale bars represent 500 nm.

## Conclusions

In conclusion, a new type of pattern doubling lithography similar to SADP, inspired by dopamine polymer chemistry, has been developed and used to produce sub-20 nm patterns. Through an immersion conformal PDA coating method, initial PMMA template pattern densities were doubled and critical feature size as low as 20 nm were produced. In addition to SADP of regular line gratings, well-defined rhombic structures were prepared. The PDA nanoscale features served as plasma

etch masks to enable the transfer of the patterns into silicon oxide substrates. To our knowledge, this work also represents the first attempt to use the carbonization from PDA pyrolysis to further reduce pattern critical dimension via shrinkage to give a further reduction of features to as low as 13 nm. Current and future work will focus on decreasing the critical size limit to < 10 nm, as well as the investigation of the electric and catalytic properties of carbonized PDA lines as suggested by the work of Li *et al.*<sup>37</sup> and Ai *et al.*<sup>37</sup> Moreover, the self-deposition of functional dopamine derivatives,<sup>41, 42</sup> post-grafting of polymers with amine- or thiol-groups to PDA,<sup>43, 44</sup> or co-deposition of PDA with other polymers<sup>45, 46</sup> would enable the incorporation of more functional groups into the sidewalls of the patterns. Through controlled etching and pyrolysis, well-tuned nano-features with a broad range of compositions, such as silicon dioxide and titanium dioxide, could potentially be achieved by this dopamine chemistry inspired self-aligned double patterning.

## Conflicts of interest

There are no conflicts to declare.

## Acknowledgements

This research was kindly supported by the NSF DMR-POLYMERS grant (DMR 1506968). This work was supported by the National Science Foundation (NSF) supported Center for Hierarchical Manufacturing (CMMI-1025020) at the University of Massachusetts, Amherst. J.C gratefully acknowledges Samsung Scholarship from the Samsung Foundation for financial support. We thank EUV Technology for kindly providing the academic license for SuMMIT software.

## References

- 1 C. Vieu, F. Carcenac, A. Pepin, Y. Chen, M. Mejias, A. Lebib, L. Manin-Ferlazzo, L. Couraud and H. Launois, *Appl. Surf. Sci.*, 2000, **164**, 111.
- 2 V. R. Manfrinato, L. H. Zhang, D. Su, H. G. Duan, R. G. Hobbs, E. A. Stach and K. K. Berggren, *Nano Lett.*, 2013, **13**, 1555.
- 3 B. Paivanranta, A. Langner, E. Kirk, C. David and Y. Ekinci, *Nanotechnology*, 2011, **22**, 375302.
- 4 V. Auzelyte, C. Dais, P. Farquet, D. Grutzmacher, L. J. Heyderman, F. Luo, S. Olliges, C. Padeste, P. K. Sahoo, T. Thomson, A. Turchanin, C. David and H. H. Solak, *J. Micro/Nanolithogr., MEMS, MOEMS*, 2009, **8**, 021204.
- 5 S. H. Park, D. O. Shin, B. H. Kim, D. K. Yoon, K. Kim, S. Y. Lee, S. H. Oh, S. W. Choi, S. C. Jeon and S. O. Kim, *Soft Matter*, 2010, **6**, 120.
- 6 S. J. Jeong, J. Y. Kim, B. H. Kim, H. S. Moon and S. O. Kim, *Mater. Today*, 2013, **16**, 468.
- 7 H. Schiff, *J. Vac. Sci. Technol., B*, 2008, **26**, 458.

- 8 M. D. Austin, H. X. Ge, W. Wu, M. T. Li, Z. N. Yu, D. Wasserman, S. A. Lyon and S. Y. Chou, *Appl. Phys. Lett.*, 2004, **84**, 5299.
- 9 J. Finders, M. Dusa, B. Vleeming, H. Megens, B. Hepp, M. Maenhoudt, S. Cheng and T. Vandeweyer, *Optical Microlithography XXI*, 2008, **6924**, 92408.
- 10 C. Bencher, Y. M. Chen, H. X. Dai, W. Montgomery and L. Huli, *Optical Microlithography XXI*, 2008, **6924**, 9244E1.
- 11 Z. N. Yu, W. Wu, L. Chen and S. Y. Chou, *J. Vac. Sci. Technol., B*, 2001, **19**, 2816.
- 12 C. H. Bak, S. J. Ku, G. C. Jo, K. Jung, H. J. Lee, S. H. Kwon and J. B. Kim, *Polymer*, 2015, **60**, 267.
- 13 C. Bencher, H. X. Dai, L. Y. Miao, Y. M. Chen, P. Xu, Y. J. Chen, S. Oemardani, J. Sweis, V. Wiaux, J. Hermans, L. W. Chang, X. Y. Bao, H. Yi and H. S. P. Wong, *Optical Microlithography XXIV*, 2011, **7973**, 79730K1.
- 14 X. M. Liu, X. G. Deng, P. Sciortino, M. Buonanno, F. Walters, R. Varghese, J. Bacon, L. Chen, N. O'Brien and J. J. Wang, *Nano Lett.*, 2006, **6**, 2723.
- 15 B. Cui, Z. N. Yu, H. X. Ge and S. Y. Chou, *Appl. Phys. Lett.*, 2007, **90**.
- 16 T. Weber, T. Kasebier, A. Szeghalmi, M. Knez, E. B. Kley and A. Tunnemann, *Microelectron. Eng.*, 2012, **98**, 433.
- 17 H. S. Moon, J. Y. Kim, H. M. Jin, W. J. Lee, H. J. Choi, J. H. Mun, Y. J. Choi, S. K. Cha, S. H. Kwon and S. O. Kim, *Adv. Funct. Mater.*, 2014, **24**, 4343.
- 18 S. M. George, *Chem. Rev.*, 2010, **110**, 111.
- 19 S. Dhuey, C. Peroz, D. Olynick, G. Calafiore and S. Cabrini, *Nanotechnology*, 2013, **24**, 105303.
- 20 A. J. M. Mackus, A. A. Bol and W. M. M. Kessels, *Nanoscale*, 2014, **6**, 10941.
- 21 M. N. Liu, X. L. Li, S. K. Karuturi, A. I. Y. Tok and H. J. Fan, *Nanoscale*, 2012, **4**, 1522.
- 22 M. Leskela and M. Ritala, *Angew. Chem., Int. Ed.*, 2003, **42**, 5548.
- 23 J. H. Waite and M. L. Tanzer, *Science*, 1981, **212**, 1038.
- 24 B. P. Lee, P. B. Messersmith, J. N. Israelachvili and J. H. Waite, *Annu. Rev. Mater. Res.*, 2011, **41**, 99.
- 25 H. Lee, S. M. Dellatore, W. M. Miller and P. B. Messersmith, *Science*, 2007, **318**, 426.
- 26 D. R. Dreyer, D. J. Miller, B. D. Freeman, D. R. Paul and C. W. Bielawski, *Chem. Sci.*, 2013, **4**, 3796.
- 27 X. C. Liu, G. C. Wang, R. P. Liang, L. Shi and J. D. Qiu, *J. Mater. Chem. A*, 2013, **1**, 3945.
- 28 B. H. Kim, D. H. Lee, J. Y. Kim, D. O. Shin, H. Y. Jeong, S. Hong, J. M. Yun, C. M. Koo, H. Lee and S. O. Kim, *Adv. Mater.*, 2011, **23**, 5618.
- 29 R. A. Zangmeister, T. A. Morris and M. J. Tarlov, *Langmuir*, 2013, **29**, 8619.
- 30 Y. H. Ding, L. T. Weng, M. Yang, Z. L. Yang, X. Lu, N. Huang and Y. Leng, *Langmuir*, 2014, **30**, 12258.
- 31 M. Y. Liu, G. J. Zeng, K. Wang, Q. Wan, L. Tao, X. Y. Zhang and Y. Wei, *Nanoscale*, 2016, **8**, 16819.
- 32 Y. Y. Li, S. X. Dai, J. John and K. R. Carter, *ACS Appl. Mater. Interfaces*, 2013, **5**, 11066.
- 33 Y. Y. Li, J. J. Peterson, S. B. Jhaveri and K. R. Carter, *Langmuir*, 2013, **29**, 4632.
- 34 F. Bernsmann, V. Ball, F. Addiego, A. Ponche, M. Michel, J. J. D. Gracio, V. Toniazzo and D. Ruch, *Langmuir*, 2011, **27**, 2819.
- 35 A. Sankaran and M. J. Kushner, *J. Vac. Sci. Technol., A*, 2004, **22**, 1242.
- 36 R. J. Li, K. Parvez, F. Hinkel, X. L. Feng and K. Mullen, *Angew. Chem., Int. Ed.*, 2013, **52**, 5535.
- 37 K. L. Ai, Y. L. Liu, C. P. Ruan, L. H. Lu and G. Q. Lu, *Adv. Mater.*, 2013, **25**, 998.
- 38 R. Liu, S. M. Mahurin, C. Li, R. R. Unocic, J. C. Idrobo, H. J. Gao, S. J. Pennycook and S. Dai, *Angew. Chem., Int. Ed.*, 2011, **50**, 6799.
- 39 W. Wei, H. W. Liang, K. Parvez, X. D. Zhuang, X. L. Feng and K. Mullen, *Angew. Chem., Int. Ed.*, 2014, **53**, 1570.
- 40 H. H. Park, W. L. Law, X. Zhang, S. Y. Hwang, S. H. Jung, H. B. Shin, H. K. Kang, H. H. Park, R. H. Hill and C. K. Ko, *ACS Appl. Mater. Interfaces*, 2012, **4**, 2507.
- 41 Y. L. Liu, K. L. Ai and L. H. Lu, *Chem. Rev.*, 2014, **114**, 5057.
- 42 Q. Ye, F. Zhou and W. M. Liu, *Chem. Soc. Rev.*, 2011, **40**, 4244.
- 43 B. D. McCloskey, H. B. Park, H. Ju, B. W. Rowe, D. J. Miller and B. D. Freeman, *J. Membr. Sci.*, 2012, **413**, 82.
- 44 O. Pop-Georgievski, D. Verreault, M. O. Diesner, V. Proks, S. Heissler, F. Rypacek and P. Koelsch, *Langmuir*, 2012, **28**, 14273.
- 45 S. M. Kang, N. S. Hwang, J. Yeom, S. Y. Park, P. B. Messersmith, I. S. Choi, R. Langer, D. G. Anderson and H. Lee, *Adv. Funct. Mater.*, 2012, **22**, 2949.
- 46 R. Zhou, P. F. Ren, H. C. Yang and Z. K. Xu, *J. Membr. Sci.*, 2014, **466**, 18.